IEEE Access
Multidisciplinary | Rapid Review | Open Access Journal

Received November 27, 2019, accepted December 2, 2019, date of publication December 6, 2019,
date of current version December 23, 2019.

Digital Object Identifier 10.1109/ACCESS.2019.2958136

Pseudo-Biological Highly Performance Transparent Electrodes Based on Capillary Force-Welded Hybrid AgNW Network

YIRU LI, BO WANG, HUAYING HU, JIANHUA ZHANG, BIN WEI, AND LIANQIAO YANG
Key Laboratory of Advanced Display and System Applications, Ministry of Education, Shanghai University, Shanghai 200072, China

Corresponding author: Lianqiao Yang (yanglianqiao@i.shu.edu.cn)

This work was financially supported by the National Natural Science Foundation of China (51505270) and the Science and Technology Committee of Shanghai (19142203600).

ABSTRACT Graphene/silver nanowire composite films have great potential as transparent conductive electrodes in the field of optoelectronic devices. So far, antioxidant and reducing the junction resistance are two major parameters in the silver nanowire electrode studies. In this paper, a pseudo-biological inspired structure for transparent electrodes was proposed by combining hybrid diameters silver nanowire network with the chemical vapor deposition-grown (CVD-grown) graphene as a passivation layer. Compared with the traditional structure, the silver nanowire network with this novel structure of human vascular tissue network greatly reduced the sheet resistance. An environmentally friendly liquid, deionized water, was selected for the generation of capillary forces at the liquid bridge, thereby improving the wire junction problem. After welding with the capillary force, the increase in the value of the figure of merit (FoM $= \sigma_{DC}/\sigma_{OP}$) acted a pivotal part in improving conductivity with excellent optical performance. In addition, graphene was chosen as an encapsulation layer to protecting silver nanowires from oxidation while improving electrical properties. Compared with the silver nanowire films with a diameter of 20 nm, the σ_{DC}/σ_{OP} of the graphene/silver nanowire composite film increased by 69.6 % with a sheet resistance of 26.4 Ω/sq. More importantly, graphene is supposed to protect silver nanowires from oxidation and moisture, which makes the composite films promising as electrodes for underwater optoelectronic devices or a possible development in high humidity environments.

INDEX TERMS Capillary force welding, graphene, hybrid diameters silver nanowire network, pseudo-biological structure.

I. INTRODUCTION

As the indispensable component of optoelectronic devices, transparent electrodes (TEs), which are widely used in organic light-emitting diodes (OLEDs), organic photovoltaic cells (OPVs), touch screens, electrochromic devices, solar cells and so on, are facing enormous challenges in order to meet the needs of human daily work life [1]–[7]. Indium tin oxide (ITO) has been the most widely used TEs as a conductive film, even though it has a series of shortcomings [8], [9]. Generally, ITO has extreme low sheet resistance ($10 \sim 20$ Ω/sq), but its transmittance is severely affected in the near-infrared wavelength range due to the high-temperature fabrication process. Moreover, the development of ITO in transparent electrodes is limited by scarce resources of indium and the complex processing flows [10], [11]. Several candidates with different dimensions expected to replace ITO have been proposed by the predecessors, including conductive polymers [12], carbon nanotubes [13], metal nanowires [14]–[16], graphene [17], [18], etc. Among these candidates, silver nanowire (AgNW) based electrodes stand out due to their excellent optoelectronic properties [19]–[21]. In addition, the fabrication process of the AgNW electrodes is simple, so that large-scale industrial production can be realized. However, there are still many problems to be solved in the practical application of AgNW electrodes.

AgNW has some innate drawbacks due to the inherent material and structures. First, AgNW films are usually made by spin coating or spraying, so that the wires are

The associate editor coordinating the review of this manuscript and approving it for publication was Derek Abbott.

just loosely stacked together at junctions, resulting in high electrical resistance. The nano-gap at the junctions hinders the transport of charge carriers and reduces the conductivity of the AgNW electrodes [22]. A series of methods for effectively improving the contact at the wire junctions have been proposed, including mechanical pressing [23], thermal heating [24], addition of soldering agents and so on [25]. However, there are many undesirable cracks generated during thermal healing process [26], [27]. Mechanical pressing destroys useful structures of AgNW films [28], and extra impurities could be introduced during the addition of soldering agents. Recently, capillary force, which is a driving force to form tightly-packed structures, has been suggested as a method for effectively welding metal nanowire films. Meng et al. reported that the mechanical property and electrical performance of In_2O_3 networks has been improved by a capillary-driven welding process [15]. This method is low cost and environmentally friendly at room temperature, which does not require any specific equipment and the soldering agent is deionized water (DI water) without introducing any impurities. During the evaporation of DI water at the junctions, capillary forces are created at the nanogaps, which are equivalent to some mechanical pressure to bind the nanowires together.

Another disadvantage of AgNW is that they are easily oxidized to AgO or Ag_2O when exposed to water or air, which results in AgNW films instability and high electrical resistance [29]. At the same time, the AgNW films exhibit a high surface roughness at the wire junctions, which generate high leakage current or even cause the devices to failure [30]. In order to overcome these two shortcomings, combining AgNW with graphene to form a graphene/AgNW composite film may be a feasible method. Firstly, as a highly conductive two-dimensional material, graphene provides more channels for charge transport, further improving the electrical properties of the composite film. Secondly, graphene can act as a passivation layer, which effectively isolates the water vapor from the AgNW and ensures the antioxidation stability of the composite electrode.

In this paper, a novel pseudo-biological stacked structure for TEs was proposed by combining two different diameters of AgNW with the CVD-grown graphene as a passivation layer. Inspired by the hierarchical structure and function of human blood vessels, hybrid nanowire electrodes were put forward, which were based on AgNW with different average diameters and lengths. Afterward, the AgNW networks were subjected to DI water for capillary welding, and the electrical properties were improved. The AgNW films were encapsulated by graphene, and the graphene/AgNW composite electrodes further improved the conductivity with negligible loss of transmittance. Moreover, the composite electrode encapsulated by graphene exhibits excellent oxidation resistance. Therefore, the composite film has great potential applicability in transparent optoelectronic devices. The fabrication procedure of graphene/AgNW composite electrodes is schematically illustrated in Figure 1.

II. EXPERIMENTAL

A. MATERIALS

All chemicals and reagents in this work were acquired from commercial sources unless otherwise noted. Silver nanowires with an average diameter of 100 nm and the length of 100∼200 μm (LDNW, nanowires with longer diameters) were purchased from Nanjing XFNANO Materials Tech. And the ones with an average diameter of 20 nm and an average length of 12 μm (SDNW, nanowires with smaller diameters) were obtained from Sigma-Aldrich.

B. FABRICATION PROCESS OF THE AgNW FILM

The SiO_2/Si substrates were washed with acetone, ethanol and DI water for 10 minutes respectively to remove impurities and organic matters from the surface. Subsequently, UV treatment was used to increase the hydrophilicity of the SiO_2/Si surface. Considering the trade balance between sheet resistance and transmittance of the electrode, it was finally determined that the concentration of LDNW was 0.8 mg/ml, and that of SDNW is 1 mg/ml. Then, two kinds of AgNW with different diameters were spin-coated on the substrate sequentially, wherein the LDNW were coated firstly. Finally, the AgNW film was welded by capillary forces. The DI water vapor was directed to the sample surface for 10s, and the distance between the jet and the sample was 5∼8 cm. Two kinds of AgNW with different diameters were stacked to form a new film, which structure just likes human vascular networks.

C. FABRICATION PROCESS OF GRAPHENE

Graphene films were synthesized by chemical vapor deposition (CVD) on an electropolished Cu foils surface using a gas mixture of Ar, H_2 and C_2H_2, where C_2H_2 was the reaction precursor. First, the copper foil (25 mm thick, 99.8 %, Alfa Aesar) was washed by electropolishing, which was a mixed solution of orthophosphoric acid (50 mL), ethanol (50 mL), isopropanol alcohol (10 mL) and urea (1 g) at the voltage of 7 V for 90s and dried with N_2 blow. Second, the dried copper foils were placed into the CVD horizontal tube furnace. The entire system was annealed under a mixed gas (H_2: Ar = 1:9) atmosphere for 30 minutes at 1000 °C. Third, 5 sccm acetylene was introduced for 15 mins, and graphene was fabricated on the Cu foils due to chemical reactions. Finally, one side of the sample was spin-coated with poly-methyl methacrylate (PMMA, Sigma-Aldrich, dissolved in chlorobenzene with a concentration of 40 mg/mL) and the other side was exposed to Ar plasma (40 W, 60 s) to obtain a single layer of graphene.

D. FABRICATION PROCESS OF THR GRAPHENE/ AgNW HYBRID FILM

The Cu foil was etched by the Marble's reagent and reserve the PMMA/graphene film. Then, the PMMA/graphene film was rinsed by DI water and transferred to the AgNW film. After removing PMMA by acetone, the graphene/AgNW

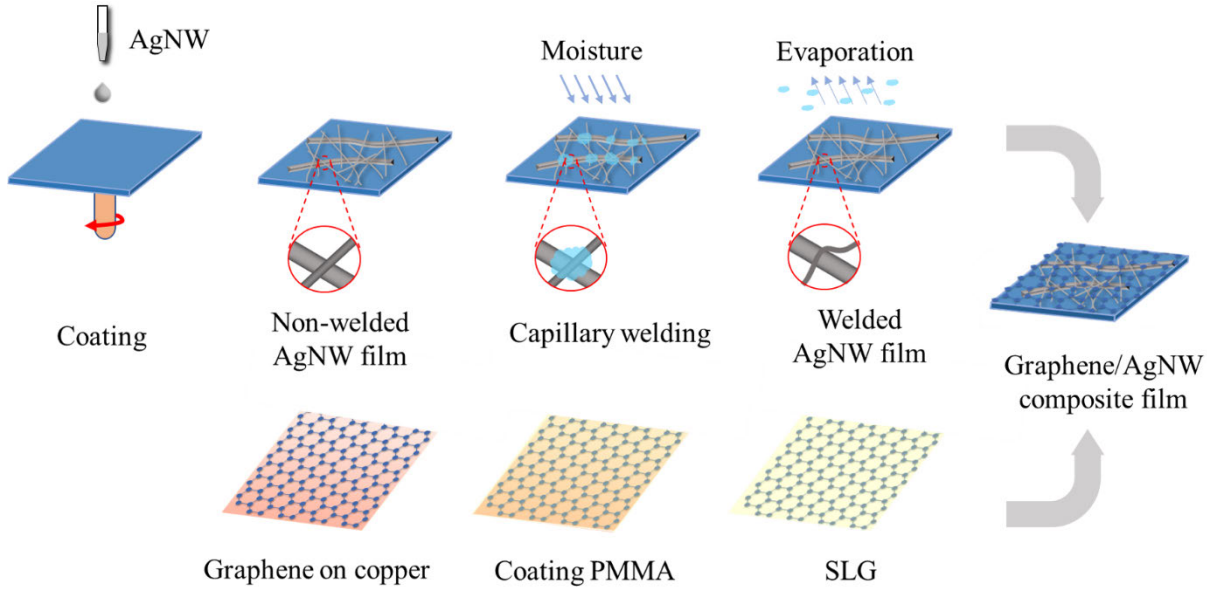

FIGURE 1. Schematic illustration of fabrication procedure of graphene/AgNW composite electrodes.

hybrid film was obtained. Finally, the sample was annealed at 120 °C in order to volatilize all solvents.

E. CHARACTERIZATIONS

Nanostructures of the composite electrodes were presented through optical microscope (KEYENCE, VHX5000), atomic force microscope (AFM, BRUKER) and field-emission scanning electron microscope (FE-SEM, Ultra 55 Zeiss). The sheet resistance of the TEs was characterized by The Hall Measurement System (ACCENT HL5550LN2). And the UV-vis spectra (U-3900H) were applied to characterize optical properties of the TEs. The Raman spectra of graphene were characterized by a Raman microscopy system (LabRAM HR XploRA) with the laser wavelength is 532 nm. During the tape test, a 10-mm-wide piece of 3M tape was used to verify the adhesion of AgNW to the substrate.

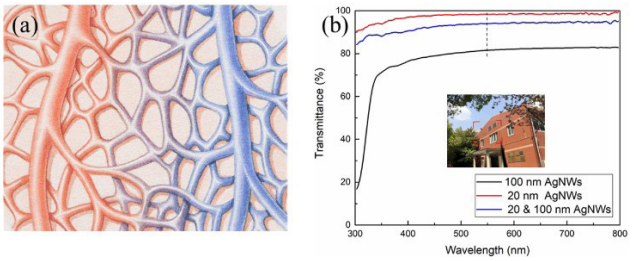

FIGURE 2. (a) The 3D model diagram of the human vascular network [31]. (b) Transmittance of AgNW films with different diameters, the inset graph is the scene through the hybrid AgNW film.

III. RESULTS AND DISCUSSION

A novel pseudo-biological structure was proposed in this paper, which likes a human vascular network. The 3D model diagram of the human vascular network was shown in Figure 2a. The human vascular network mainly includes: arteries, veins and capillaries, in which the arteries and veins are relatively thick blood vessels, while the capillaries are relatively thin blood vessels. Arteries, veins, and capillaries perform their duties. The diameter of the arteries and veins is larger, so the flow rate of blood is fast and unimpeded. In contrast, capillaries with a smaller diameter are distributed widely and bring blood vessels to subtle tissues. This structure was applied to the AgNW film in this paper, which means a hybrid film of AgNW with different diameters (HDNW, hybrid nanowires with different diameters). The LDNW with better electron transport properties were responsible for most of the charge movement. At the same time, there were fewer junctions in the network formed with the LDNW due to its longer length. As shown in Figure S1, we selected the minimum critical path for the transmission of the two kinds of silver nanowires in the AgNW film, and labeled the number of nodes. It can be seen that there were fewer junctions in the network formed with the LDNW obviously. Similar results can also be found in the previous literature [32]. While the SDNW filled the lacunae that uncovered by LDNW, making the entire film more oriented toward a two-dimensional plane. On another aspect, the film filled by the SDNW became denser, which is more conducive to charge collection in device applications. Therefore, TEs with this human vascular inspired structure has great prospects in device manufacturing.

In addition, the photoelectric property was improved by adopting this human-like vascular structure. Figure 2b showed the transmittance of AgNW films with different diameters. It is seen clearly that the transmittance of LDNW film was only 80.6 % at 550 nm, which is much lower than the SDNW ones (98.4 %). However, the sheet resistance of SDNW networks was 288 Ω/sq, while the sheet resistance of the LDNW ones was only 13 Ω/sq. Therefore, we selected

their respective advantages and spin-coated AgNW films with this pseudo-biological structure, which greatly reduced the sheet resistance with little loss of the transmission. The transmittance of hybrid AgNW film increased to 94.5 %, which was nearly 14 % higher than the transmittance of the film composed of the LDNW. The inset graph of Figure 2b shows the scene through the hybrid AgNW film on glass; the red dotted rectangular shows the area of the sample with the size of 3×2.5 cm^2. No vision disparity is observed in the graph, which also confirms the uniformity and transparency of the hybrid films.

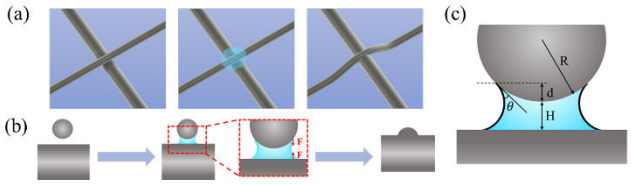

FIGURE 3. (a, b) Schematic illustration of the welding process for AgNW networks. (c) Schematic of the mechanism of capillary interaction between a sphere and a plate connected with a liquid bridge.

The AgNW films formed by spin-coating were fabricated with weak wire connections at the junctions, which led to instability and high electrical resistance. Figure 3a and b show the principle that the capillary soldering process applied in AgNW networks can effectively improve the contact problem of junctions. Obviously, there were nanogaps at the wire junctions, which formed positions with large mean curvature [33]. The Kell equation predicts that liquid prefers to condense at these nanogaps [34]. By the process of directing water vapor onto the surface of AgNW films, the condensation occurred and a wire-to-wire liquid bridge was formed to connect AgNW together [35]. The sample was dried naturally in the air, and the strong capillary force was generated at junctions, and finally the purpose of welding AgNW was achieved during subsequent liquid evaporation. The capillary force between nanowires was mainly composed of two parts: the F_1 generated at the corners between the silver nanowires and the substrate, the F_2 generated at junctions between nanowires. The F_1 was calculated by the equation 1 [36]:

$$F_1 = 2D\gamma\left(\frac{\cos\theta_1 + \cos\alpha}{\tan\varphi} + \sin\alpha\right) \tag{1}$$

where $\alpha = \theta_2 + \varphi, D$ is the diameter of the AgNW. θ_1 and θ_2 are water contact angles on the substrate and AgNW respectively. ϕ is the angle between the silver nanowire and the substrate. On the other hand, the diameter of the SDNW was only 1/5 of the LDNW one, therefore the LDNW can be approximated as a plane compared to the SDNW at the junction position. We assumed the structure at junctions as a model of a sphere and a plate connected by a liquid bridge (Figure 3c). The capillary force can be estimated by the following equation 2 [37]:

$$F_2 = -\frac{4\pi\gamma R\cos\theta}{1 + H/d} \tag{2}$$

where R is the radius of the sphere, which is approximately equal to the radius of the AgNW; γ represents liquid surface tension, and the value of water is 72.8 mN/m at room temperature; H is the closest distance of the sphere to the plate; θ is the contact angle; d is the immersion length and can be calculated by the following equation 3:

$$d = -H + \sqrt{H^2 + V/(\pi R)} \tag{3}$$

where V is the liquid volume; the value of V and θ is 1×10^3 nm^3 and 60° respectively in a typical case. Through the above formula, the capillary force F_1 was calculated to be 15.12 nN. The distance H between AgNW at junctions was considered as 5 nm, and the actual measured value is less than 1 nm from the AFM (Figure 8a). The value of capillary force was calculated to be about 1.97 nN, and increased gradually as the separation distance decreases. AgNW were tightly compressed together through the capillary force. Moreover, the capillary welding is self-limiting. That is, when the welding is completed, the gap between the wires disappears so that there is almost no capillary force generated at this position. Theoretically, the AgNW networks can be welded effectively by this method.

The fact that the AgNW network was effectively welded by the capillary force has been demonstrated by SEM images. In Figure 4a, the non-welding AgNW was spin-coated onto the substrate and simply stacked together. No deformation occurred at junctions, and there were many nanogaps between AgNW. In contrast, Figure 4b showed the surface topography of the welded AgNW network. The SDNW on the top had undergone severe deformation and embedded in the LDNW deeply. The deformation was easily seen through a magnification SEM image of an individual junction location (Figure 4c). However, at the junctions where the AgNW with the same diameter intersected in Figure 4b, the deformation was very inconspicuous and AgNW did not appear to be connected together. In order to verify that the welding effect of the hybrid AgNW networks proposed in this paper was better than the AgNW networks with the same diameter, we performed the same welding process for the AgNW with diameters of 100 nm and 20 nm respectively. As shown in Figure 4d, the AgNW film consisting solely of LDNW had no significant difference before and after welding, which was clearly seen from the enlarged single-junction SEM image (Figure 4e). Similarly, the welding effect of the SDNW was not obvious, and there were only few junctions welded (Figure 4f). Therefore, it was further explained that such an AgNW network using a human blood vessel network structure was more easily welded to reduce the looseness of the junctions.

Considering the actual application of electrode in optoelectronic devices, the AgNW electrode should meet certain mechanical requirements to ensure stability. As shown in Figure 5, the tapping test was used to evaluate the mechanical properties of the AgNW electrode with or without the welding process [38]. A piece Scotch tape (3M) was pressed

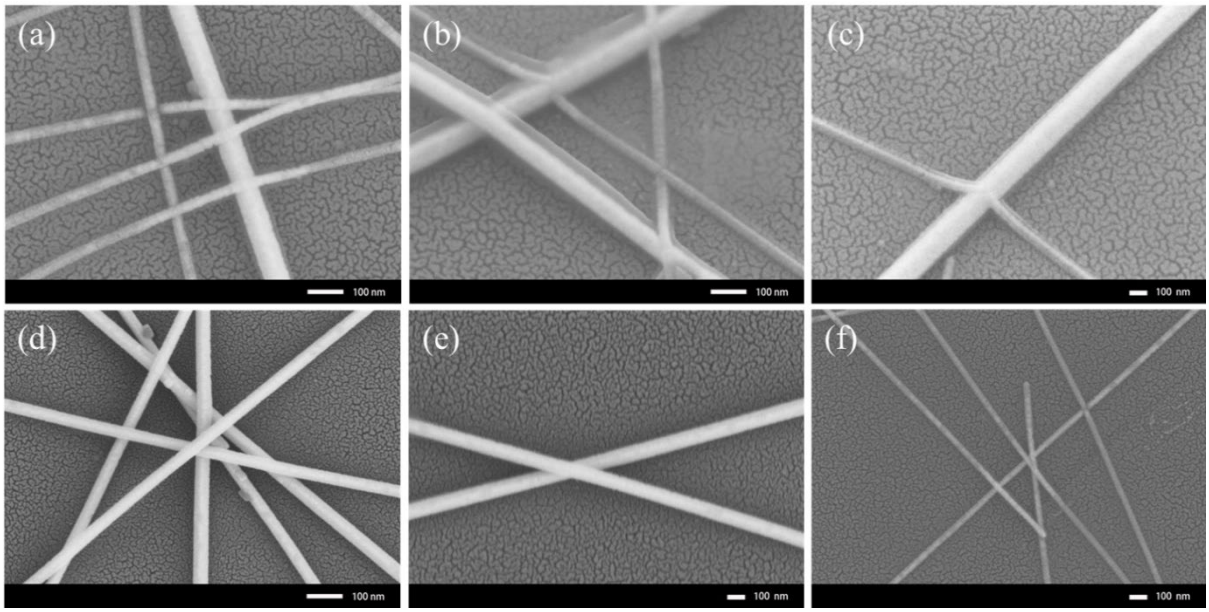

FIGURE 4. (a) SEM microimage of non-welded AgNW network with the human blood vessel network structure. (b) Low- and (c) high-magnification SEM images of welded AgNW network with the human blood vessel network structure. (d) Low- and (e) high-magnification SEM images of the welded LDNW network. (f) SEM microimage of the welded SDNW.

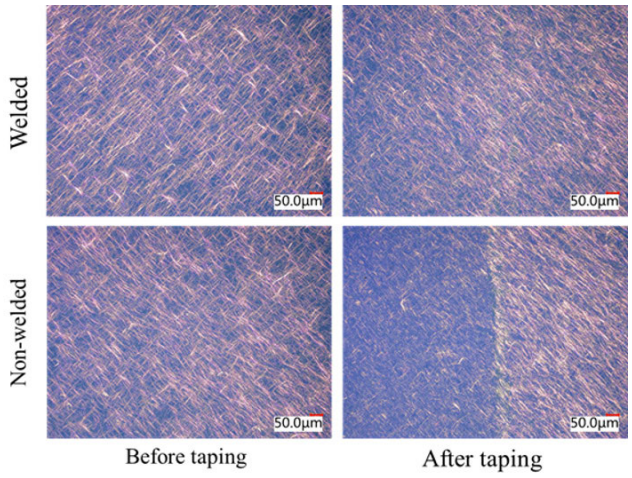

FIGURE 5. Tapping tests of AgNW with/without welding process.

against the surface of the AgNW film, and then pulled away from the film. The optical microscope was used to observe the adhesion of the sample on the substrate. The stickiness of the tape made it easy for the non-welding AgNW to fall off during this process. In contrast, in the AgNW films with welded, the density of AgNW reduced by a very small amount. There was significant improvement compared to the non-welded sample. Therefore, it was confirmed that the welding process enhanced the adhesion of the AgNW to the substrate, which is consistent with the previous report [39]. This ensures the survival of the AgNW film during fabrication of the composite electrode in the subsequent wet transfer of graphene.

It is well-known that AgNW is easily oxidized to AgO or Ag_2O when exposed to water or air. In order to enhance antioxidation stability, graphene was used to encapsulate the hybrid AgNW film. The graphene used in this composite electrode was synthesized by copper-catalyzed CVD method. During the growth process, the graphene grew on both sides of the copper foil [40]. The presence of graphene on the back of the copper foil affected the subsequent process, such as etching the copper foil and graphene transfer processes, thereby affected the performance of the single-layer graphene (SLG). The quality and numbers of graphene layers affect the resistance and transmittance of the composite electrode deeply [41]. As shown in Figure S2a, there were many extra strips on the transferred graphene, resulting in a decrease in transmittance and an increase in surface roughness [42]. Therefore, it is necessary to remove the graphene on the backside of the copper foil. By optimizing the Radio Frequency (RF) process, the appropriate parameters are determined (RF power: 40 W, time: 60 s). Of course, excessive RF power and overtime cleaning would cause the graphene film to be damaged. As shown in the Figure S2c, there were many cracks on the graphene film, which reduced the electrical properties of graphene. Conversely, if the cleaning time was insufficient or the RF power was too low, it would result in cleaning incompletely (Figure S2d). After exposing to Ar plasma for 60 s, smooth and flat SLG was obtained (Figure S2b).

The Raman spectra, average Raman spectra of 3 points of graphene on the SiO_2/Si substrate (Figure 6a), further verified the effect of plasma treatment. The shift of the three typical peaks of graphene was not obvious: D peak ($\sim$1350 cm^{-1}), G peak ($\sim$1580 cm^{-1}) and 2D peak ($\sim$2700 cm^{-1}). However, the D peak decreased significantly, even almost disappeared, which indicated there were few defects of graphene [43].

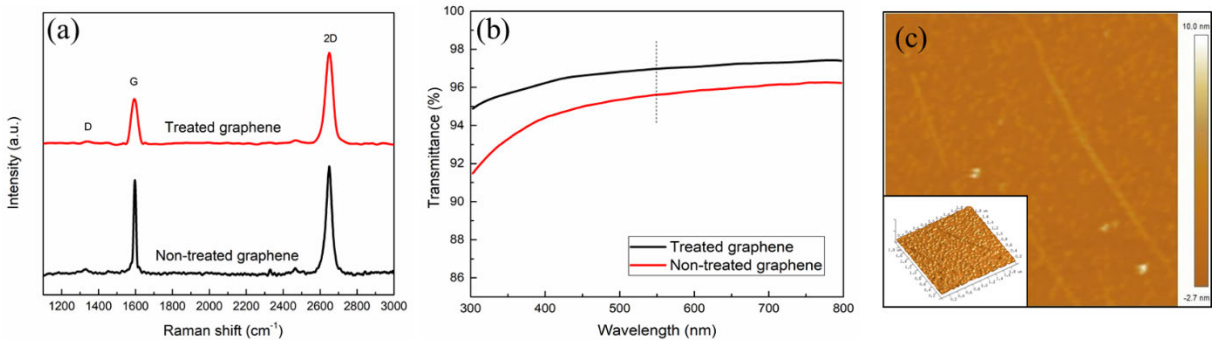

FIGURE 6. (a) Raman spectra and (b) transmittance of CVD-grown graphene. (c) AFM image and height profile of the SLG with size 2 × 2 μm and its 3D image.

At the same time, the ratio of the intensity of the G and 2D peak (I_G/I_{2D}) decreased after plasma treatment. The I_G/I_{2D} is about 0.5, and the half-width of the 2D peak is about 33 cm^{-1}, which presents typical features of SLG [44]. Moreover, the transmittance of the graphene increased to 97 % at the wavelength of 550 nm after cleaning treatment (Figure 6b). As one layer of TEs, high transmittance is extremely important for transparent optoelectronic device.

As shown in Figure 6c, the roughness of the graphene was just 0.8 nm, which was not much different from ITO (RMS = 0.7 nm) [45]. It is easy to find there were some inevitable wrinkles on the surface, which designed to maintain its thermodynamic stability, just like many other 2D materials [46]. These wrinkles would cause the failure of optoelectronics when graphene is used as an electrode alone [22]. Unbelievable, when graphene is transferred to the AgNW network, some of the wrinkles occurred and wrapped around the AgNW tightly, increasing the surface contact area and enhancing adhesion [47]. Therefore, these wrinkles bond the graphene, the AgNW and the substrate together closely, which reduced the roughness of the composite electrode and increased the adhesion of the electrode to the substrate.

Generally, the two factors of sheet resistance and transmittance mutually restrict each other [47]. The figure of merit (FoM = σ_{DC}/σ_{OP}) was proposed to balance the transmittance and the sheet resistance as equation 4 [48], [49]:

$$\frac{\sigma_{DC}}{\sigma_{OP}} = \frac{Z_0}{2R_S\left(T^{-\frac{1}{2}} - 1\right)} \tag{4}$$

where σ_{DC} is direct current; σ_{OP} is optical conductivity; Z_0 is the impedance of free space (377 Ω); R_S and T are sheet resistance and transmittance, respectively. The high value of the σ_{DC}/σ_{OP} means higher transmittance and low sheet resistance. As shown in Figure 7, it was seen that the FoM of the TEs consisted of only a single diameter of silver nanowires was at small value (< 80), even if the LDNW electrode had a lower sheet resistance. The FoM of the hybrid AgNW film with the pseudo-biological structure reached 92.5 with low sheet resistance. Furthermore, after the AgNW film was welded and encapsulated by graphene, the ratio

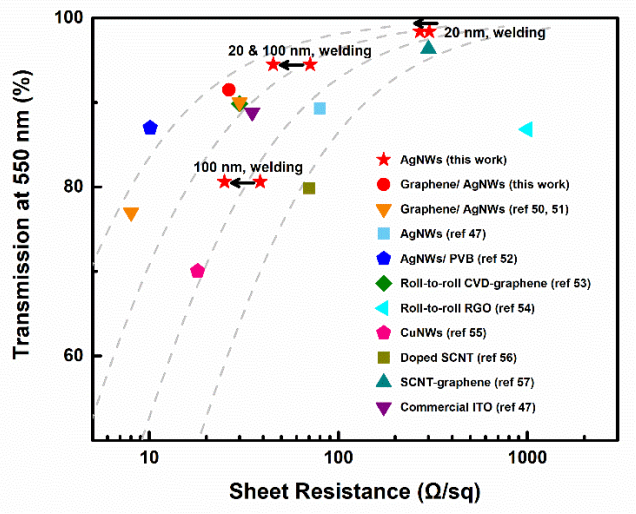

FIGURE 7. Sheet resistance versus optical transmission at 550 nm of different TEs. The dotted line inside indicates four different values of FoM = 25, 50, 100 and 200. The data at both ends of the arrow represent the performance of the electrode before and after welding.

was further increased to 145.3 and 157.0 respectively. The sheet resistance of the composite film was finally maintained at 26.4 Ω/sq, which demonstrated this novel structure was more suitable of the composite electrodes with better optoelectronic performance. Subsequently, the electrodes were compared with other transparent conductive electrodes that have been reported, including graphene/AgNWs [50], [51], AgNWs [47], AgNWs/ PVB [52], roll-to-roll CVD-graphene [53], roll-to-roll RGO [54], CuNW [55], doped SCNT [56], SCNT-graphene [57] and commercial ITO [47]. The results show that the graphene/ AgNWs composite electrode reported herein showed a relatively lower square resistance with higher transmittance. There were some reported electrodes with higher FoM than ours, but long-term stability or worse transparency may be factors limiting possible application. Moreover, in our paper, we demonstrated that the performance of the composite film with this new structure exhibited much better performance than that of the original films in many aspects. The significance of this study was to

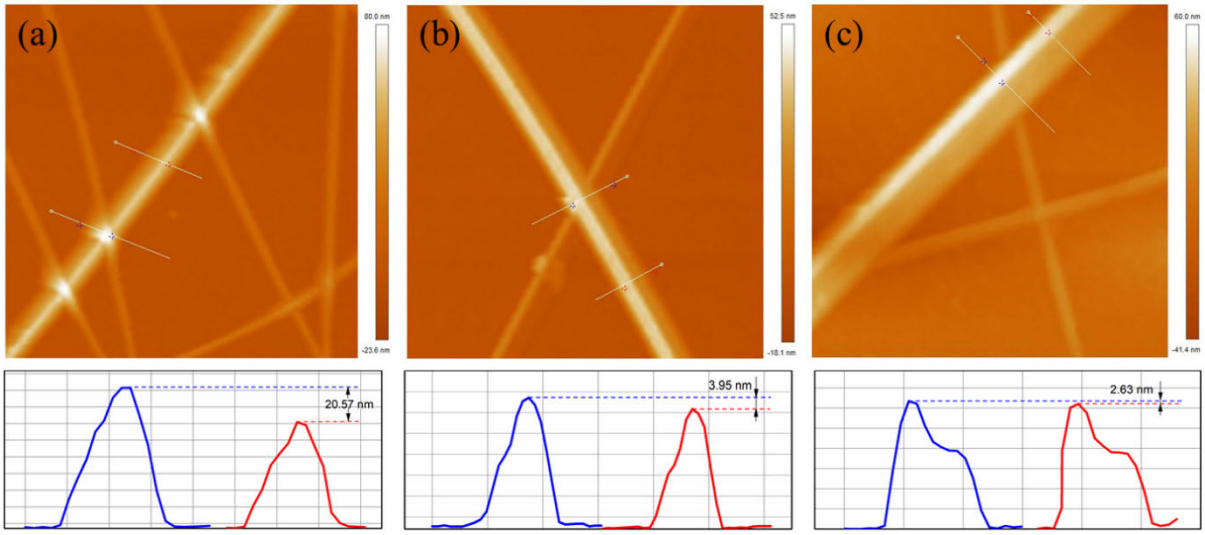

FIGURE 8. AFM images, height profile of (a) the non-welding AgNW network, (b) the welded AgNW network, and (c) the AgNW/graphene composite film. Low magnification SEM images of (d) the AgNW network and (e) the AgNW/graphene composite film with size 2 × 2 μm.

provide a possibility for the structure of the silver nanowire or other materials composite electrodes.

The welding process also effectively reduced the surface roughness of the AgNW networks. One of the ways to reduce the risk of leakage current of the device is to flatten the surface. The surface roughness of the welded AgNW was 7.4 nm, which was reduced by 3.9 nm compared with the non-welded films. Moreover, the surface roughness of the AgNW/graphene composite film was further reduced [58], and finally reached 6.4 nm. The possible reasons were explained as follows: First, graphene was grown on copper substrates. The surface morphology of the copper substrate does not match the target SiO_2/Si substrate. The AFM image of the single layer of graphene showed that there were some typical line defects such as wrinkles and ripples in the graphene on the SiO_2/Si substrate [59]. In the silver nanowire films, there were a lot of inevitable gaps between the silver nanowires, resulting in similar surface morphology to the copper substrate. Therefore, the silver nanowire acted as a ''buffer'' to release the structural deformation of the graphene [60], and finally the flatter composite film was obtained. In addition, the height difference between wire junctions and the lines further confirmed the effectiveness of the welding process. As shown in Figure 8a, the height difference between the junction and the line was 20.57 nm, which was slightly larger than the diameter of the SDNW. The height difference reduced to 3.95 nm (Figure 8b), which was significantly smaller than the diameter. Finally, Figure 8c shows the height difference of the AgNW/graphene composite film was only 2.63 nm, which fully demonstrated that the composite film was flat enough to be suitable for the transparent optoelectronic devices.

Moisture resistance is one of the essential factors for the commercialization of TEs. Simultaneously, the graphene in the composite film acted as a protective layer for the AgNW. Under the protection of graphene passivation layers, AgNW/graphene based TEs exhibited excellent moisture resistance. During tests and applications, AgNW was inevitably exposed to the air, and the two main factors affecting the stability are oxygen and moisture. The granular objects observed in both AFM (Figure S3) and SEM (Figure 9a) images were predicted to be oxides of AgNW. However, such granular objects had not been found in the AFM (Figure 8c) and SEM (Figure 9b) image of the AgNW/graphene composite film. The XPS of the two kinds of films further proved this conjecture. Three distinct peaks were shown in Figure S4, in which the two peaks at 373.4 eV and 367.4 eV represent the presence of Ag in the form of Ag $3d_{3/2}$ and Ag $3d_{5/2}$, respectively. The peak at 367.8 eV was the characteristic peak of Ag_2O, which indicated that part of the silver nanowires was oxidized in the AgNW films (Figure S4a) [61]. In comparison, the peak intensity at 367.8 eV was significantly reduced in the AgNW/graphene films (Figure S4b).

In order to further verify the effect of graphene on protecting AgNW from moisture, we conducted the following experiment: a thin strip of AgNW/graphene composite electrode on glass was connected to a circuit in the atmosphere, and applied to illuminate the LED light (Figure 9c). Next, the AgNW/graphene electrode was immersed in DI water for more than 24 hours, and then illuminated the LED lamp again (Figure 9d). It can be seen that the composite electrode was not destroyed by prolonged exposure to moisture. The brightness of the LED lamp hardly changed, which indicated that the oxidation and shedding of composite electrodes protected by graphene were negligible. This provides a possibility for optoelectronic devices to develop in high humidity environments and even underwater devices.

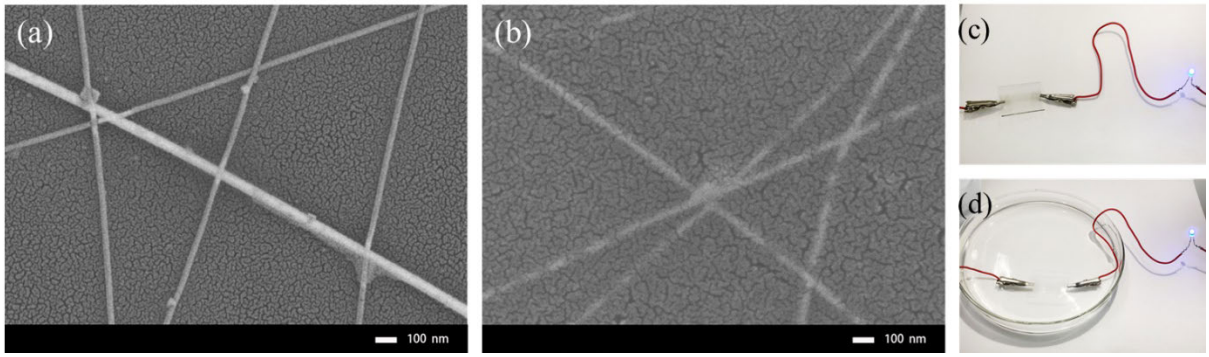

FIGURE 9. Low magnification SEM images of (a) the AgNW network and (b) the AgNW/graphene composite film with size 2 × 2 μm. Luminescence experiment of LEDs connected by composite electrodes in (c) atmosphere, (d) DI water.

IV. CONCLUSION

In conclusion, we proposed a novel pseudo-biological stacked structure as TEs, that is, a network composing of two different diameters of AgNW combined with CVD-grown graphene as a passivation layer. This new structure was introduced to improve conductivity with negligible loss of transmission. The AgNW film was effectively welded by capillary force and the conductivity ratio was increased to 145.26. As an encapsulation layer, graphene effectively slowed the oxidation of AgNW and provided more channels for charge transport. The conductivity ratio of the graphene/AgNW composite film increased to 157.04 with the square resistance of 26.4 Ω/sq. Moreover, the surface roughness of the composite film was 6.4 nm, which was about 5 nm lower than that of the original AgNW network. Hence, it has great potential to be applied in optoelectronic devices in high humidity environments and even underwater devices due to its flat surface, excellent optical and electrical properties, and long-term stability.

REFERENCES

[1] Y. H. Kahng, M.-K. Kim, J.-H. Lee, Y. J. Kim, N. Kim, D.-W. Park, and K. Lee, "Highly conductive flexible transparent electrodes fabricated by combining graphene films and inkjet-printed silver grids," *Sol. Energy Mater. Solar Cells*, vol. 124, no. 5, pp. 86–91, Feb. 2014.

[2] H. Sun, G. Ge, J. Zhu, H. Yan, Y. Lu, Y. Wu, J. Wan, M. Han, and Y. Luo, "High electrical conductivity of graphene-based transparent conductive films with silver nanocomposites," *RSC Adv.*, vol. 5, no. 130, pp. 108044–108049, May 2015.

[3] B. Liu, C. Li, Q.-L. Liu, J. Dong, C.-W. Guo, H. Wu, H.-Y. Zhou, X.-J. Fan, X. Guo, C. Wang, X.-M. Sun, Y.-H. Jin, Q.-Q. Li, and S.-S. Fan, "Hybrid film of silver nanowires and carbon nanotubes as a transparent conductive layer in light-emitting diodes," *Appl. Phys. Lett.*, vol. 106, no. 3, p. 2779, Jan. 2015.

[4] T. H. Seo, A. H. Park, S. Park, S. Chandramohan, G. H. Lee, M. J. Kim, C.-H. Hong, and E.-K. Suh, "Improving the graphene electrode performance in ultra-violet light emitting diode using silver nanowire networks," *Opt. Mater. Express*, vol. 5, no. 2, p. 314, Jan. 2015.

[5] C. D. Yun, K. Hyun Wook, S. Hyung Jin, and K. S. Soo, "Annealing-free, flexible silver nanowire-polymer composite electrodes via a continuous two-step spray-coating method," *Nanoscale*, vol. 5, no. 3, pp. 977–983, 2013.

[6] S. Shuai, L. Wang, P. Song, L. Ding, and Y. Bai, "Facile fabrication of hydrolysis resistant phosphite antioxidants for high-performance optical PET films via *in situ* incorporation," *Chem. Eng. J.*, vol. 328, no. 15, pp. 406–416, Nov. 2017.

[7] Z. Zhang, J. Du, D. Zhang, H. Sun, L. Yin, L. Ma, J. Chen, D. Ma, H. M. Cheng, and W. Ren, "Rosin-enabled ultraclean and damage-free transfer of graphene for large-area flexible organic light-emitting diodes," *Nature Commun.*, vol. 8, Feb. 2017, Art. no. 14560.

[8] O. Inganäs, "Organic photovoltaics: Avoiding indium," *Nature Photon.*, vol. 5, no. 4, pp. 201–202, 2011.

[9] J. L. Miao, H. H. Liu, C. B. Li, and X. X. Zhang, "Graphene-based film reduced by a chemical and thermal synergy method as a transparent conductive electrode," *Sci. Adv. Mater.*, vol. 8, no. 5, pp. 1066–1073, 2016.

[10] A. Yabuki, K. Okumura, and I. W. Fathona, "Transparent conductive coatings of hot-pressed ITO nanoparticles on a plastic substrate," *Chem. Eng. J.*, vol. 252, no. 252, pp. 275–280, 2014.

[11] J. Yang, B. Wang, Y. Zhang, X. Ding, and J. Zhang, "Low-temperature combustion synthesis and UV treatment processed p-type Li: NiO X active semiconductors for high-performance electronics," *J. Mater. Chem. C*, vol. 6, no. 46, pp. 12584–12591, 2018.

[12] M. Vosgueritchian, D. J. Lipomi, and Z. Bao, "Highly conductive and transparent PEDOT: PSS films with a Fluorosurfactant for stretchable and flexible transparent electrodes," *Adv. Funct. Mater.*, vol. 22, no. 2, pp. 421–428, 2012.

[13] O. Reynaud, A. G. Nasibulin, A. S. Anisimov, I. V. Anoshkin, J. Hua, and E. I. Kauppinen, "Aerosol feeding of catalyst precursor for CNT synthesis and highly conductive and transparent film fabrication," *Chem. Eng. J.*, vol. 255, no. 6, pp. 134–140, 2014.

[14] S. Cho, S. Kang, A. Pandya, R. Shanker, Z. Khan, Y. Lee, J. Park, S. L. Craig, and H. Ko, "Large-area cross-aligned silver nanowire electrodes for flexible, transparent, and force-sensitive mechanochromic touch screens," *ACS Nano*, vol. 11, no. 4, pp. 4346–4357, Apr. 2017.

[15] Y. Meng, K. Lou, R. Qi, Z. Guo, B. Shin, G. Liu, and F. Shan, "Nature-inspired capillary-driven welding process for boosting metal-oxide nanofiber electronics," *ACS Appl. Mater. Interfaces*, vol. 10, no. 24, pp. 20703–20711, Jun. 2018.

[16] M. J. Large, M. Cann, S. P. Ogilvie, A. A. King, I. Jurewicz, and A. B. Dalton, "Finite-size scaling in silver nanowire films: Design considerations for practical devices," *Nanoscale*, vol. 8, no. 28, p. 13701, Jul. 2016.

[17] H. H. Jin, H. S. Dong, S. Kim, H. J. Min, H. L. Min, W. S. Sang, S. H. Choi, and H. I. Sang, "Highly efficient $CH_3NH_3PbI_3$ perovskite solar cells prepared by $AuCl_3$-doped graphene transparent conducting electrodes," *Chem. Eng. J.*, vol. 323, pp. 153–159, Sep. 2017.

[18] K. K. Soo, Z. Yue, J. Houk, L. S. Yoon, K. J. Min, K. S. Kim, A. Jong-Hyun, K. Philip, C. Jae-Young, and H. B. Hee, "Large-scale pattern growth of graphene films for stretchable transparent electrodes," *Nature*, vol. 457, no. 7230, pp. 706–710, Feb. 2009.

[19] B. Li, S. Ye, I. E. Stewart, S. Alvarez, and B. J. Wiley, "Synthesis and purification of silver Nanowires to make conducting films with a transmittance of 99," *Nano Lett.*, vol. 15, no. 10, p. 6722, 2015.

[20] B. Wei, X. Wu, L. Lian, S. Yang, D. Dong, D. Feng, and G. He, "A highly conductive and smooth AgNW/PEDOT:PSS film treated by hot-pressing as electrode for organic light emitting diode," *Organic Electron.*, vol. 43, pp. 182–188, Jan. 2017.

[21] M. J. Large, J. Burn, A. A. King, S. P. Ogilvie, I. Jurewicz, and A. B. Dalton, "Predicting the optoelectronic properties of nanowire films based on control of length polydispersity," *Sci. Rep.*, vol. 6, p. 25365, May 2016.
[22] X.-Y. Zeng, Q.-K. Zhang, R.-M. Yu, and C.-Z. Lu, "A new transparent conductor: Silver nanowire film buried at the surface of a transparent polymer," *Adv. Mater.*, vol. 22, no. 40, pp. 4484–4488, Oct. 2010.
[23] S. Ye, A. R. Rathmell, Z. Chen, I. E. Stewart, and B. J. Wiley, "Metal nanowire networks: The next generation of transparent conductors," *Adv. Mater.*, vol. 26, no. 39, pp. 6670–6687, 2014.
[24] J. Y. Lee, S. T. Connor, Y. Cui, and P. Peumans, "Solution-processed metal nanowire mesh transparent electrodes," *Nano Lett.*, vol. 8, no. 2, p. 689, 2008.
[25] J. Lee, P. Lee, H. B. Lee, S. Hong, I. Lee, J. Yeo, S. S. Lee, T. S. Kim, D. Lee, and S. H. Ko, "Silver nanowires: Room-temperature nanosoldering of a very long metal nanowire network by conducting-polymer-assisted joining for a flexible touch-panel application," *Adv. Funct. Mater.*, vol. 23, no. 34, pp. 4171–4176, 2014.
[26] L. Yang, H. J. Yu, W. Chao, S. Shouheng, and L. Jun, "Cold welding of ultrathin gold nanowires," *Nature Nanotechnol.*, vol. 5, no. 3, pp. 218–224, 2010.
[27] M. E. T. Molares, A. G. Balogh, T. W. Cornelius, R. Neumann, and C. Trautmann, "Fragmentation of nanowires driven by Rayleigh instability," *Appl. Phys. Lett.*, vol. 85, no. 22, pp. 5337–5339, 2004.
[28] Y. Liu, J. Zhang, H. Gao, Y. Wang, Q. Liu, S. Huang, C. F. Guo, and Z. Ren, "Capillary-force-induced cold welding in silver-nanowire-based flexible transparent electrodes," *Nano Lett.*, vol. 17, no. 2, pp. 1090–1096, Feb. 2017.
[29] D. Li, W. Y. Lai, Y. Z. Zhang, and W. Huang, "Printable transparent conductive films for flexible electronics," *Adv. Mater.*, vol. 30, no. 10, 2018, Art. no. 1704738.
[30] G. Whitney, G. F. Burkhard, M. D. Mcgehee, and P. Peter, "Smooth nanowire/polymer composite transparent electrodes," *Adv. Mater.*, vol. 23, no. 26, p. 2904, 2011.
[31] (1995). *VCG: Diagram Of Capillary Network Running Between Arteriole And Venule*. [Online]. Available: https://www.vcg.com/creative/1008395697
[32] X. Wang, R. Wang, H. Zhai, L. Shi, and J. Sun, "Leaf vein' inspired structural design of Cu nanowire electrodes for the optimization of organic solar cells," *J. Mater. Chem. C*, vol. 6, no. 21, pp. 5738–5745, 2018.
[33] M. Kohei, H. Siya, I. Mitsumasa, and P. Wei, "Enhanced conductivity and gating effect of p-type Li-doped NiO nanowires," *Nanoscale*, vol. 6, no. 2, pp. 688–692, 2013.
[34] L. R. Fisher and J. N. Israelachvili, "Direct experimental verification of the Kelvin equation for capillary condensation," *Nature*, vol. 277, no. 5697, pp. 548–549, 1979.
[35] S. S. Yoon and D. Y. Khang, "Room-temperature chemical welding and sintering of metallic Nanostructures by capillary condensation," *Nano Lett.*, vol. 16, no. 6, p. 3550, 2016.
[36] K. Zhang, J. Li, Y. Fang, B. Luo, Y. Zhang, Y. Li, J. Zhou, and B. Hu, "Unraveling the solvent induced welding of silver nanowires for high performance flexible transparent electrodes," *Nanoscale*, vol. 10, no. 27, pp. 12981–12990, Jul. 2018.
[37] Y. I. Rabinovich, M. S. Esayanur, and B. M. Moudgil, "Capillary forces between two spheres with a fixed volume liquid bridge: Theory and experiment," *Langmuir*, vol. 21, no. 24, pp. 10992–10997, 2005.
[38] L. Lian, D. Dong, S. Yang, B. Wei, and G. He, "Highly conductive and uniform alginate/silver nanowire composite transparent electrode by room temperature solution processing for organic light emitting diode," *Acs Appl. Mater. Inter.*, vol. 9, no. 13, pp. 11811–11818, 2017.
[39] H. Li, C. Zhu, J. Xue, Q. Ke, and Y. Xia, "Enhancing the mechanical properties of Electrospun nanofiber mats through controllable welding at the cross points," *Macromol. Rapid Commun.*, vol. 38, no. 9, 2017, Art. no. 1600723.
[40] H. Zhou, W. J. Yu, L. Liu, R. Cheng, Y. Chen, X. Huang, Y. Liu, Y. Wang, Y. Huang, and X. Duan, "Chemical vapour deposition growth of large single crystals of monolayer and bilayer graphene," *Nat. Commun.*, vol. 4, p. 2096, Jun. 2013.
[41] S. B. Yang, H. Choi, D. S. Lee, C. G. Choi, S. Y. Choi, and I. D. Kim, "Improved optical sintering efficiency at the contacts of silver nanowires encapsulated by a graphene layer," *Small*, vol. 11, no. 11, pp. 1293–1300, Mar. 2015.
[42] J. Miao, H. Liu, W. Li, and X. Zhang, "Mussel-inspired polydopamine-functionalized graphene as a conductive adhesion promoter and protective layer for silver nanowire transparent electrodes," *Langmuir*, vol. 32, no. 21, pp. 5365–5372, May 2016.
[43] K. Hyungki, S. Intek, P. Chibeom, S. Minhyeok, H. Misun, K. Youngwook, K. J. Sung, S. Hyun-Joon, B. Jaeyoon, and C. H. Cheul, "Copper-vapor-assisted chemical vapor deposition for high-quality and metal-free single-layer graphene on amorphous SiO_2 substrate," *ACS Nano*, vol. 7, no. 8, pp. 6575–6582, 2013.
[44] Y. Zhang, L. Zhang, P. Kim, M. Ge, Z. Li, and C. Zhou, "Vapor trapping growth of single-crystalline graphene flowers: Synthesis, morphology, and electronic properties," *Nano Lett.*, vol. 12, no. 6, pp. 2810–2816, 2012.
[45] G. D. A. Lewis, Z. Yi, C. W. Schlenker, R. Koungmin, M. E. Thompson, and Z. Chongwu, "Continuous, highly flexible, and transparent graphene films by chemical vapor deposition for organic photovoltaics," *Acs Nano*, vol. 4, no. 5, pp. 2865–2873, 2010.
[46] F. Liu, J. Choi, and T. Seo, "Graphene oxide arrays for detecting specific DNA hybridization by fluorescence resonance energy transfer," *Biosensors Bioelectron.*, vol. 25, no. 10, pp. 2361–2365, 2010.
[47] J. Miao, S. Chen, H. Liu, and X. Zhang, "Low-temperature nanowelding adherent ultrathin silver nanowire sandwiched between polydopamine-functionalized graphene and conjugated polymer for highly stable and flexible transparent electrodes," *Chem. Eng. J.*, vol. 345, pp. 260–270, Aug. 2018.
[48] S. De and J. N. Coleman, "Are there fundamental limitations on the sheet resistance and transmittance of thin graphene films?" *ACS Nano*, vol. 4, pp. 2713–2720, May 2010.
[49] L. Shi, J. Yang, T. Yang, Q. Hanxun, J. Li, and Q. Zheng, "Molecular level controlled fabrication of highly transparent conductive reduced graphene oxide/silver nanowire hybrid films," *RSC Adv.*, vol. 4, no. 81, pp. 43270–43277, 2014.
[50] J. Trevithick, J. Li, T. R. Ohno, and C. A. Wolden, "Activation of CdTe solar cells using molecular chlorine," in *Proc. IEEE 43rd Photovoltaic Spec. Conf. (PVSC)*, Portland, OR, USA, May 2016, pp. 0518–0523.
[51] X. Zhang, V. A. Öberg, J. Du, J. Liu, and E. M. J. Johansson, "Extremely lightweight and ultra-flexible infrared light converting quantum dot solar cells with high power-per-weight output using a solution-processed bending durable silver nanowire based electrode," *Energy & Environ. Sci.*, vol. 11, no. 2, pp. 354–364, 2018
[52] L. Lu, X. Xin, D. Dan, and G. He, "Highly conductive silver nanowire transparent electrode by selective welding for organic light emitting diode," *Organic Electron.*, vol. 60, pp. 9–15, Sep. 2018.
[53] S. Bae, H. Kim, Y. Lee, X. Xu, J. S. Park, Y. Zheng, J. Balakrishnan, T. Lei, H. R. Kim, Y. I. Song, and Y. J. Kim, "Roll-to-roll production of 30-inch graphene films for transparent electrodes," *Nature Nanotechnol.*, vol. 5, no. 8, pp. 574–578, Jun. 2010.
[54] J. Ning, L. Hao, M. Jin, X. Qiu, Y. Shen, J. Liang, X. Zhang, B. Wang, X. Li, and L. Zhi, "A facile reduction method for roll-to-roll production of high performance graphene-based transparent conductive films," *Adv. Mater.*, vol. 29, no. 9, 2017, Art. no. 1605028.
[55] S. Han, S. Hong, J. Ham, J. Yeo, J. Lee, B. Kang, P. Lee, J. Kwon, S. S. Lee, and M.-Y. Yang, "Fast plasmonic laser nanowelding for a Cu-nanowire percolation network for flexible transparent conductors and stretchable electronics," *Adv. Mater.*, vol. 26, no. 33, pp. 5808–5814, 2014.
[56] H.-Z. Geng, K. K. Kim, K. P. So, Y. S. Lee, Y. Chang, and Y. H. Lee, "Effect of acid treatment on carbon nanotube-based flexible transparent conducting films," *J. Amer. Chem. Soc.*, vol. 129, no. 25, pp. 7758–7759, 2007.
[57] S. H. Kim, W. Song, M. W. Jung, M.-A. Kang, K. Kim, S.-J. Chang, S. S. Lee, J. Lim, J. Hwang, and S. Myung, "Carbon nanotube and graphene hybrid thin film for transparent electrodes and field effect transistors," *Adv. Mater.*, vol. 26, no. 25, pp. 4247–4252, Jul. 2014.
[58] Y. Ge, X. Duan, M. Zhang, L. Mei, J. Hu, W. Hu, and X. Duan, "Direct room temperature welding and chemical protection of silver nanowire thin films for high performance transparent conductors," *J. Amer. Chem. Soc.*, vol. 140, no. 1, 2017, Art. no. jacs.7b07851.
[59] G. X. Ni, Y. Zheng, S. Bae, H. R. Kim, A. Pachoud, Y. S. Kim, C.-L. Tan, D. Im, J.-H. Ahn, and B. H. Hong, "Quasi-periodic nanoripples in graphene grown by chemical vapor deposition and its impact on charge transport," *ACS Nano*, vol. 6, no. 2, pp. 1158–1164, 2012.
[60] Z. Chen, X. Xu, J. Zhang, M. Shin, and L. Yang, "Highly transparent conductive films fabricated by combining CVD-grown graphene and silver nanowire," *Mol. Cryst. Liq. Cryst.*, vol. 651, no. 1, pp. 250–258, 2017.

[61] S. H. Kim, W. I. Choi, K. H. Kim, D. J. Yang, S. Heo, and D. J. Yun, "Nanoscale chemical and electrical stabilities of graphene-covered silver nanowire networks for transparent conducting electrodes," *Sci. Rep.*, vol. 6, p. 33074, Sep. 2016.

YIRU LI was born in Hebei, China, in September 27, 1993. She is currently pursuing the master's degree with the School of Material Science and Engineering, Shanghai University, Shanghai, China. She is currently with the Key Laboratory of Advanced Display and System Applications, Ministry of Education, Shanghai University. Her current research interest includes transparent electrodes for OLED devices based on graphene composite films.

BO WANG was born in Anhui, China, in October 28,1993. He is currently pursuing the master's degree with the Microelectronics Research and Design Center, Shanghai University. He is currently with the Key Laboratory of Advanced Display and System Applications, Ministry of Education, Shanghai University. His current research interest includes biosensors based on graphene for the detection of organophosphate pesticides.

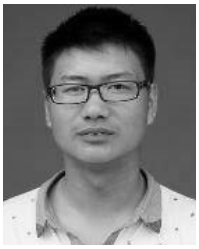

HUAYING HU is currently pursuing master's degree with the School of Material Science and Engineering, Shanghai University. He is currently with the Key Laboratory of Advanced Display and System Applications, Shanghai University. His main research interests include the applications of graphene in biosensor for the detection of organophosphorus pesticides from water and agricultural products, and immunosensor for the detection of AFP (alpha fetoprotein) from human body.

JIANHUA ZHANG is a Professor of photoelectronic and mechanical engineering with Shanghai University, Shanghai, China. She is the Head of the Light-Emitting Diode (LED) and Organic Light-Emitting Diode (OLED) Center and the Director of the Key Laboratory for Advance Display Technology and System Applications, Ministry of Education, Shanghai University. Her current research interests include high-power LEDs, OLED devices, and thin film technology.

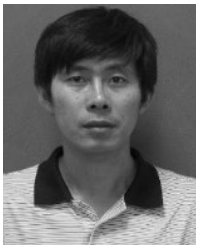

BIN WEI is a Professor of photoelectronic and mechanical engineering with Shanghai University, Shanghai, China. He is the Vice Director of the Key Laboratory for Advance Display Technology and System Applications, Ministry of Education, Shanghai University. His current research interest includes advanced materials and their applications in organic optoelectronic devices.

LIANQIAO YANG was born in Hebei, China, in 1979. She received the B.S. degree from Wuhan University, Wuhan, China, in 2004, and the M.S. and Ph.D. degrees from Myongji University, Seoul, South Korea, in 2006 and 2009, respectively. She joined Shanghai University, Shanghai, China, in 2009. Her current research interests include the thermal management of opto-electronics and the development of advanced materials.